Identification of Residues on CD40 and Its Ligand Which Are Critical for the Receptor−Ligand Interaction†

Jürgen Bajorath,*,‡ N. Jan Chalupny,‡ John S. Marken,‡ Anthony W. Siadak,‡ John Skonier,‡ Marcia Gordon,‡ Diane Hollenbaugh,‡ Randolph J. Noelle,§ Hans D. Ochs,|| and Alejandro Aruffo‡

Bristol-Myers Squibb Pharmaceutical Research Institute, Seattle, Washington 98121, Department of Microbiology, Dartmouth Medical School, Lebanon, New Hampshire 03756, and Department of Pediatrics, University of Washington School of Medicine, Seattle, Washington 98195

Received August 23, 1994; Revised Manuscript Received October 28, 1994⊗

ABSTRACT: Interactions between gp39 (CD40L, TRAP, T-BAM) on activated T cells and CD40 on antigen-presenting cells play an important role in regulating antibody production by B cells, cytokine production by monocytes, and other immune responses which require T cell "help". Using structure-based sequence alignments, a molecular model of gp39, site-directed mutagenesis, and receptor−ligand binding assays, we have identified CD40 and gp39 surface residues which are important for receptor−ligand binding. Binding studies with CD40 or gp39 proteins containing single and double amino acid substitutions showed that CD40 residues Y82, D84, and N86 are involved in gp39 binding, while gp39 residues K143 and Y145 are important for CD40 binding. Analysis of the location of amino acid substitutions in the naturally occurring gp39 mutants expressed by the X-linked hyper-IgM (X-HIM) patients studied to date indicated the E129/G substitution found in the S128/R-E129/G double mutant affects a solvent-accessible residue which might participate in CD40/gp39 binding. Binding studies with E129/G and E129/A gp39 point mutants showed that this residue does not contribute directly to CD40/gp39 binding but that its substitution with a glycine disrupts the gp39 structure. Comparison of the gp39 and CD40 residues involved in receptor−ligand contacts with those previously identified as playing an important role in TNF-β/TNFR binding suggests that some of the identified residues form contacts similar to those found in the TNF-β/TNFR while others are unique to the CD40−gp39 interaction.

T cell mediated "help" is an essential component of a productive immune response. In recent years a number of cell surface proteins expressed by activated T helper cells (T_h) have been implicated as important mediators of T cell help. Gp39 (CD40L, TRAP, T-BAM) (Armitage et al., 1992; Hollenbaugh et al., 1992; Spriggs et al., 1992; Lederman et al., 1994a; Graf et al., 1992; Lane et al., 1992; Hermann et al., 1993), a type II membrane protein expressed by activated T cells, has been shown to be one of these proteins. *In vitro*, the anti-murine gp39 mAb[1] MR1 can block T cell dependent B cell proliferation (Noelle et al., 1992) and antibody synthesis (Foy et al., 1993). Similar results have been obtained with the anti-human gp39 mAb 5C8 (Lederman et al., 1992, 1994b). *In vivo*, MR1 has been shown to block antibody response against T cell dependent antigens (Foy et al., 1993; Van den Eertwegh et al., 1993) and collagen-induced arthritis (Durie et al., 1993). The effects of MR1 and 5C8 *in vitro* and MR1 *in vivo* are thought to be due to the ability of these antibodies to block the interaction of gp39 with its receptor, CD40, a type I membrane protein expressed by antigen-presenting cells (APC) (Clark & Ledbetter, 1986; Paulie et al., 1985). Isolation of a cDNA clone encoding CD40 showed that this protein is a member of the tumor necrosis factor receptor gene family (Stamenkovic et al., 1988).

Isolation of cDNA clones encoding murine (Armitage et al., 1992) and human gp39 (Graf et al., 1992; Hollenbaugh et al., 1992; Spriggs et al., 1992; Lederman et al., 1994a) has shown that the extracellular domain of this protein is homologous to tumor necrosis factor (TNF) [for recent reviews, see Smith et al., (1994) and Hollenbaugh et al. (1994)]. The availability of a cDNA clone encoding gp39 allowed the preparation of a soluble recombinant form of the protein (sgp39) which was used to examine the role of gp39 in B lymphocyte and macrophage activation. These studies showed that in the presence of a costimulus sgp39 can drive B cell proliferation (Hollenbaugh et al., 1992; Lane et al., 1993) and antibody production (Nonoyama et al., 1993) as well as cytokine production by adherent macrophages (D. Hollenbaugh and P. Kiener, unpublished). The effects of sgp39 could be blocked with CD40-Ig, a soluble recombinant form of CD40. Similar effects, but without the requirement for a costimulus, can be obtained with membrane-bound gp39 (Armitage et al., 1992; Spriggs et al., 1992; Alderson et al., 1993).

Perhaps the most compelling evidence for the role of gp39 in T cell help in humans comes from the recent finding that

†This work was supported by NIH Grants HD-17427 (H.D.O.) and AI-26296 (R.J.N.), a grant from the Arthritis Foundation to R.J.N., a grant from the March of Dimes Birth Defects Foundation (6-0116) to H.D.O., and the Bristol-Myers Squibb Pharmaceutical Research Institute.

* Address correspondence to this author at BMS-PRI, 3005 First Ave., Seattle, WA 98121 [telephone (206) 727-3612; Fax (206) 727-3602].

‡ Bristol-Myers Squibb Pharmaceutical Research Institute.

§ Dartmouth Medical School.

|| University of Washington School of Medicine.

⊗ Abstract published in *Advance ACS Abstracts,* January 1, 1995.

[1] Abbreviations: APC, antigen-presenting cells; CD40-Ig, CD40 immunoglobulin fusion protein; ELISA, enzyme-linked immunosorbent assay; HRP, horseradish peroxidase; mAb, Monoclonal antibody; PCR, polymerase chain reaction; sgp39, soluble recombinant gp39; TNF, tumor necrosis factor; X-HIM, hyper-IgM syndrome.

0006-2960/95/0434-1833$09.00/0

naturally occurring defects in gp39 are responsible for X-linked hyper-IgM syndrome (X-HIM) (Aruffo et al., 1993; Allen et al., 1993; Korthauer et al., 1993; Di Santo et al., 1993; Fuleihan et al., 1993). Affected males have normal or elevated levels of circulating IgM but no detectable serum IgG, IgA, or IgE. The inability of these patients to mount an effective humoral immune response against T cell dependent antigens renders them susceptible to opportunistic infections. Peripheral blood B cells from these individuals are normal and can proliferate and isotype switch in response to CD40 stimulation with anti-CD40 mAb or sgp39 (Aruffo et al., 1993; Durandy et al., 1993).

Presently, little is known about the molecular contacts which are responsible for the gp39−CD40 binding. However, substantial information exists on the molecular interaction between TNF and TNFR. The crystal structures of TNF-α and -β have been reported (Eck & Sprang, 1989; Eck et al., 1992; Jones et al., 1989) as has the structure of the TNF-β/TNFR complex (Banner et al., 1993). This information and data obtained from multiple mutagenesis and binding studies have allowed the identification of amino acid residues in the extracellular domain of TNF which are critical for receptor binding. The availability of the atomic coordinates for TNF-α through the Brookhaven Protein Data Base made it possible to prepare a three-dimensional model of gp39 (Aruffo et al., 1993). Here we describe the use of this model and the reported crystallographic contacts (linkage map) of the TNF-β/TNFR complex to select a number of gp39 and CD40 extracellular domain residues with putative involvement in receptor−ligand contacts. We also examined the predicted location of naturally occurring gp39 mutations found in the defective gp39 genes of the patients with X-HIM syndrome studied to date. Affected residues were classified as being buried or surface-accessible. It would be expected that mutations of buried residues may compromise the gp39 tertiary and/or quaternary structure resulting in protein which can no longer interact with CD40. In contrast, mutations of surface-accessible residues are less likely to affect the protein structure and may directly affect critical gp39−CD40 contacts. Site-directed mutagenesis experiments and receptor−ligand binding assays were used to examine the role of particular amino acids in gp39−CD40 binding.

MATERIALS AND METHODS

Cell Lines, Fusion Proteins, and Antibodies. The B cell line Daudi was obtained from the ATCC (Rockville, MD). The T cell line BMS-10 was a gift of Dr. R. Mittler (Bristol-Myers Squibb, Seattle, WA). The wild-type soluble CD40-Ig, Leu 8-Ig, sgp39 and sCD72 have been previously described (Noelle et al., 1992; Hollenbaugh et al., 1992; Walz et al., 1990). The anti-murine mAb 53-6 and the anti-CD40 mAb G28-5 were a gift from Dr. J. Ledbetter (Bristol-Myers Squibb, Seattle, WA). The biotinylated anti-murine CD8 mAb Ly-2 was obtained from Caltag Laboratories (San Francisco, CA). The anti-human CD40 and gp39 mAbs 40−1.87, 40−2.210, 40−2.131, 40−1.62, 39−1.26, 39−1.59, 39−1.124, 39−1.156, and 39−7.3 will be described elsewhere (Siadak et al., in preparation).

Selection of CD40 and gp39 Residues Targeted for Substitution. Residues targeted for mutagenesis on gp39 and CD40 were selected on the basis of a previously derived comparative protein model of the gp39 extracellular region (Aruffo et al., 1993), on the basis of structure-based sequence alignments of gp39 vs TNF-β and CD40 vs TNFR, respectively, and on the basis of the reported crystallographic contacts in the TNF-β/TNFR complex structure (Banner et al., 1993). Computer graphics analysis of the gp39 model was carried out using Insight II (BIOSYM Technologies Inc., San Diego, CA) on a Silicon Graphics Indigo workstation. Sequences were initially aligned using the GCG programs (Genetics Computer Group Inc., Madison, WI) and manually modified, taking three-dimensional information and constraints of the TNF-β (Eck et al., 1992) and the TNF-β/TNFR crystal (Banner et al., 1993) structures into account.

Construction of CD40 and gp39 Mutants. Amino acid substitutions and silent mutations for diagnostic restriction enzyme sites were introduced into cDNA fragments encoding the extracellular domains of either CD40 or gp39 by using an overlap extension PCR protocol (Ho et al., 1989) as previously described. The CD40-Ig fusion genes were prepared by subcloning the PCR-amplified CD40 extracellular domain mutants into the mammalian expression vector CDM7B$^-$ which contained a cDNA fragment encoding the hinge, CH2, and CH3 domains of human IgG1 (Noelle et al., 1992). The fusion genes encoding the mutant sgp39 proteins were prepared by subcloning the PCR-amplified gp39 extracellular domain mutants into the same mammalian expression vector containing a cDNA fragment encoding the extracellular domain of murine CD8 (Lyt2a) (Hollenbaugh et al., 1992). The PCR primers used for the CD40 constructs are as follows: CD40 forward primers, 5′ GCGAAGCTTATGGTTCGTCTGCCTCTGCAGTGC 3′ and 5′ GCGCTCGAGATGGTTCGTCTGCCTCTGCAGTGC 3′; CD40 Reverse Primer, 5′ CGCCGGATCCTGGGGACCACAGACAACATCAGTCTTGTTTGTGCC 3′; CD40 mutant primers, (R73/A) 5′ GGTGAAAGCGAATTTCTAGACACCTGGAACGCAGAGACACACTGCCACC 3′, (H76/A) 5′ GGTGAAAGCGAATTTCTAGACACCTGGAACAGAGACAGCCTGCCACCAGCACAAATACTGC 3′, (Y82/A) 5′ CACCAGCACAAAGCCTGCGACCCCAACCTAGGGCTACGCGTCCAGCAGAAGGGC 3′, (D84/A) 5′ CAGCACAAATACTGCGCCCCCAACCTAGGGCTACGCGTCCAGCAGAAGGGC 3′, (N86/A) 5′ CACAAATACTGCGACCCCGCCCTAGGGCTACGCGTCCAGCAGAAGGGC 3′, (S113/A) 5′ GGCTGGCACTGTACGGCTGAAGCTTGTGAGAGCTGTGTCC 3′, and (E114/A) 5′ GGCTGGCACTGTACTAGTGCGGCCTGTGAGAGCTGTGTCC 3′. The forward and reverse PCR primers used for the gp39 constructs have been previously described (Hollenbaugh et al., 1992). The PCR primers used for the gp39 mutants areas follows: (E129/A) 5′ AATCCTCAAAATGCGGCACATGTGATCAGTGCGGCCAGCAGTAAAACAACA 3, (S131/A-T135/A) 5′ CAAAATGCGGCACATGTGATCAGTGAGGCCGCCAGTAAAACAGCATCTGTGTTACAGTGGGCT 3′, (K143/A) 5′ AGTAAAACAACATCTGTGCTGCAGTGGGCTGAAGCAGGATACTACACCATGAGC 3′, (Y145/A) 5′ AGTAAAACAACATCTGTGCTGCAGTGGGCTGAAAAAGGAGCCTACACCATGAGCAACACT 3′, (N180/A) 5′ CAAGTCACCTTCTGTTCCGCTCGGGAGGCTTCGAGTCAAGCTCCA 3′, (F201/A-E202/A) 5′ AGCCTCTGCCTAAAGTCCCCCGGGAGAGCCGCGAGAATCTTACTCAGAGCT 3′, and (N240/A-D243/A) 5′ GGTGCATCGGTGTTTGTCGCTGTGACTGCTCCGTCTCAAGTGAGCCATGGCACT 3′. The corresponding reverse primers are the reverse complement of the sequences listed above. Base changes that encode the alanine are shown

in bold type. The diagnostic restriction sites added or deleted are underlined. Forward (for) and reverse (rev) PCR oligos for the gp39−S128/R and gp39−E129/G mutants are as follows: (S128/R-rev) 5′ GATGTTGTTTTACTGGAAGCTTCTCTTAT GACATGTGC 3′, (S128/R-for) 5′ CATGTCATAAGAGAAGCTTCCAGTAAA ACAACATCTG, and (E129/G-rev) 5′ GATGTTGTTTTACTGCTGGCTCCGGATATGACATGTGCC 3′, and (E129/G-for) 5′ CATGTCATATCCGGAGCCAGCAGTAAAACAACATCTG 3′. Base changes that encode the amino acid substitutions are shown in bold type. The diagnostic restriction sites added or deleted are underlined.

Production and Characterization of Wild-Type and Mutant CD40 and gp39 Proteins. Wild-type and mutant CD40 and sgp39 proteins were produced from transiently transfected COS cells as described elsewhere (Hollenbaugh et al., 1992; Noelle et al., 1992). For SDS−PAGE analysis of the COS cell supernatants, 1×10^7 transfected COS cells were metabolically labeled with [^{35}S]methionine and [^{35}S]cysteine (Tran^{35}S-Label, ICN, Costa Mesa, CA) 25 h post transfection for a 24-h period. The CD40-Ig fusion proteins were recovered by immunoprecipitation with immobilized protein A (Repligen Corp., Cambridge, MA). The sgp39 proteins were immunoprecipitated from the supernatant of transfected COS cells with the anti-murine CD8 mAb 53-6 followed by anti-rat Ig antibodies conjugated to Sepharose. The immunoprecipitated proteins were analyzed by SDS−PAGE (8% for CD40-Ig and 10% for sgp39) under reducing conditions.

Binding of Wild-Type and Mutant CD40-Ig to BMS-10 Cells in Solution. BMS-10 cells, a Jurkat cell line variant which expresses surface gp39, were incubated with wild-type or mutant CD40-Ig or a control fusion protein, Leu 8-Ig (25 μg/mL, 1 h, room temperature), followed by FITC-conjugated goat anti-human IgG Fc (1:500 dilution, 30 min, room temperature; TAGO, Burlingame, CA). Fusion protein binding to 5×10^5 cells was analyzed by flow cytometry (FACscan, Becton Dickinson, Mountain View, CA).

Binding of Wild-Type and Mutant CD40-Ig to Immobilized sgp39. The wells of 96-well plates (Immunolon-2, Dynatech, Chantilly, VA) were coated with the anti-murine CD8 mAb G53-6 (5 μg/mL, 1 h, room temperature), blocked with 1× specimen diluent (1 h, room temperature; Genetic Systems, Seattle, WA), washed, and incubated with neat COS cell supernatant containing the sgp39 (1 h, room temperature). Wells were washed three times and incubated with wild-type or mutant CD40-Igs (starting at a concentration of 10 μg/mL and titrated down with serial 1:2 dilutions in PBS for 1 h, room temperature). Wells were washed five times and incubated with HRP-conjugated goat F(ab′)$_2$ anti-human IgG Fc (1:10 000, 1 h, room temperature; Jackson Immunoresearch, West Grove, PA). Wells were washed five times, and the plate was developed with the chromogenic substrate TMB (Genetic Systems chromogen diluted 1:100 in EIA-buffered substrate, Genetic Systems). The reaction was stopped after 15 min with the addition of 1 N H_2SO_4, and the absorbance was measured on an ELISA reader at dual wavelengths, 450 and 630 nm.

Binding of Immobilized Wild-Type and Mutant CD40-Igs to BMS-10 Cells. Cell binding assays with wild-type and mutant CD40-Igs were carried out as previously described (Hollenbaugh et al., 1993) using BMS-10 cells.

Binding of Wild-Type and Mutant sgp39 to Daudi Cells. The ability of wild-type and sgp39 to bind to CD40 expressed on Daudi cells was assayed by flow cytometry . Briefly, 0.5×10^5 log phase Daudi cells, which had been preincubated with human IgG to block Fc receptors (10 mg/mL; Sigma, St. Louis, MO), were incubated with 100 μL of COS cell supernatants containing the sgp39 proteins (1 h, room temperature). After washing, cells were incubated with 100 μL of PBS + 2% FBS + 1 μg/mL human IgG (binding buffer) and a 1:50 dilution of the biotin-conjugated rat anti-murine CD8 mAb Ly-2 (1 h, room temperature; Caltag Laboratories, San Francisco, CA). The cells were washed and incubated in 100 μL of binding buffer containing 1:500 dilution of fluorescein-conjugated avidin (1 h, room temperature; Molecular Probes, Eugene, OR). After washing, the cells were analyzed by flow cytometry. To ensure that the binding studies were not affected by variable amounts of sgp39 proteins in the different COS cell supernatants, titration experiments were performed using serially diluted COS cell supernatants.

Binding of Immobilized Wild-Type and Mutant sgp39 to CD40-Ig. Methods for purifying active sgp39 have not been established; therefore a capture assay was used in which wild-type and mutant sgp39 were captured from COS cell supernatants using the anti-murine CD8 mAb 53-6 (10 μg/mL, 1 h, room temperature) adsorbed to the wells of a 96-well plate (Immunolon-2, Dynatech, Chantilly, VA). Following antibody coating the plates were blocked with 1× specimen diluent (1 h, room temperature). After washing five times, neat gp39 COS cell supernatants containing wild-type or mutant sgp39 in DMEM/2% FBS were added to the plate and incubated for 2 h at room temperature. The plates were washed, and serial dilutions of CD40-Ig (100 μL/well, initial CD40-Ig concentration was 50 μg/mL) in PBS with 2% FBS were added to each well and incubated for 1 h at room temperature. The plates were washed and incubated with 100 μL/well of a1:9000 HRP-conjugated rat anti-human IgG antibody (Jackson Laboratory, Bar Harbor, ME) for 1 h at room temperature. After washing, bound HRP-conjugated antibody was assayed as previously described. The plates were read at dual wavelengths, 450 and 630 nm.

To ensure that equal amounts of each sgp39 protein were immobilized on the plates for the CD40-Ig binding assays, the amount of sgp39 in each well was quantitated as follows. COS cell supernatants containing the different proteins were incubated on plates coated with the anti-murine mAb 53-6. The levels of captured sgp39 were then monitored using a biotin-conjugated anti-murine CD8 mAb Ly-2, which was found to recognize an epitope distinct from that recognized by mAb 53-6. On the basis of the quantitation data obtained from these experiments, the amount of mAb 53-6 used to coat the wells was adjusted appropriately to ensure that saturating, and therefore equivalent, amounts of each of the sgp39 proteins were used in the binding experiments.

RESULTS

CD40 and gp39 Structure-Based Sequence Alignment. Recently, the crystal structure of the 55-kDa form of the TNFR complexed to one of its ligands, TNF-β, was reported (Banner et al., 1993). On the basis of this report we prepared a structure-oriented sequence alignment of CD40 and TNFR (Figure 1A). Because of the low sequence identity between these two molecules (domains 2 and 3 of TNFR display <30% sequence identity with their corresponding domains in CD40), the alignment was centered at residues which were shown crystallographically to be characteristic of the TNFR

(A)

```
      62                    *     *           *   *   *   88
CD40: C G E S E F L D T W N R E T H C H Q H K Y C D P N L G
TNFR: C E S G S F T A S E N H L R H C L S C S K C R K E M G
      55                                                  81
                                                          *
                                    (104)                 * 114
CD40: L R V Q Q K G T S E T D T I C T C E E G - W H C T S E
TNFR: Q V E I S S C T V D R D T V C G C R K N Q Y R H Y W S
                                                          108

                                                          140
CD40: A C E S - C V L H R S C S P G F G V K Q I A T G V S D
TNFR: E N L F Q C F N C S L C L N G - T V H L S C Q E K Q N
                                                          134

            144
CD40: T I C E
TNFR: T V C T
            138
```

(B)

```
      125   * *   *       *                 *   *         151
gp39: H V I S E A S S K T T S V L Q W A E K G Y Y T M S N N
TNFß: H L I G D P S - K Q N S - L L W R A N T D R A F L Q D
      32                                                  56

                                                          178
gp39: L V T L E N G K Q L T V K R Q G L Y Y I Y A Q V T F C
TNFß: G F S L S N - N S L L V P T S G I Y F V Y S Q V V F S
                                                          82

        *                                                 200
gp39: S N R E A - - - - S S Q A P F I A S L C L K S P - G R
TNFß: G K A Y S P K A T S S P L Y L A H E V Q L F S S Q Y P
                                                          109

      * *                                                 226
gp39: F E R I L L R A A N T H S S - A K P C G Q Q S I H L G
TNFß: F H V P L L S S Q K M V Y P G L Q E P W L H S M Y H G
                                                          136

                                  *     *                 253
gp39: G V F E L Q P G A S V F V N V T D P S Q V S H G T G F
TNFß: A A F Q L T Q G D Q L S T H T D G I P H L V L S P S T
                                                          163
```

FIGURE 1: CD40/TNFR and gp39/TNF-β structure-based sequence alignment. (A) Structure-based sequence alignment of the extracellular domain of CD40 versus the extracellular domain of the 55-kDa form of TNFR. (B) Structure-based sequence alignment of the extracellular domain of gp39 versus the extracellular domain of TNF-β. Residues targeted for replacement are shown (•). Conserved residues are shown in bold. Sequence homologies for the regions included in the CD40/TNFR alignment and the gp39/TNF-β alignment are approximately 26% and 25%, respectively.

structure. These residues include those involved in the formation of disulfide bonds and residues within the core regions of this molecule. Many of these TNFR residues were found to be conserved or conservatively replaced in CD40. These observations provide further evidence of the structural similarity between CD40 and TNFR, which is reflected in the assignment of corresponding (or topologically equivalent) residue positions in the sequence–structure alignment. Banner et al. (1993), who determined the crystal structure of the TNF-β/TNFR complex, generated a linkage diagram of the TNF-β/TNFR contacts by calculating the reduction of the solvent-accessible surface of the two proteins upon complex formation. In the absence of a three-dimensional model of CD40, this structure-oriented alignment was combined with the TNF-β/TNFR linkage map to select CD40 residues for mutagenesis.

A similar approach was used in the generation of a structure-based alignment of gp39 with TNF-β (Figure 1B). This alignment, in conjunction with analysis of our previously reported three-dimensional model of the gp39 homotrimer (Aruffo et al., 1993; Bajorath et al., 1993), allowed the identification of a number of gp39 residues predicted to be topologically equivalent to solvent-accessible residues in the TNF-β X-ray structure, which, due to their location and

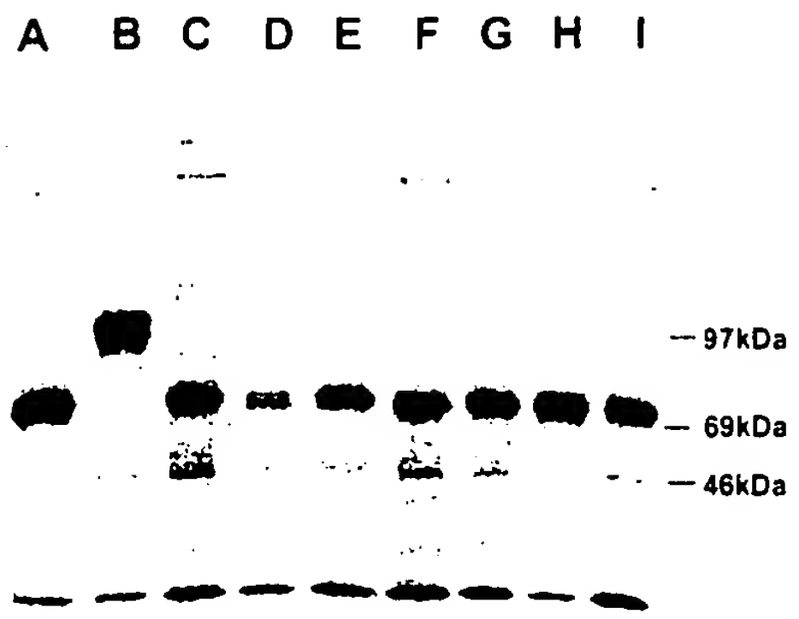

FIGURE 2: Wild-type and mutant CD40-Ig proteins. SDS–PAGE analysis of wild-type and mutant proteins obtained from the supernatant of COS cell transfectants: (A) wild-type CD40-Ig, (B) control fusion protein Leu 8-Ig, (C) CD40-R73/A, (D) CD40-H76/A, (E) CD40-Y82/A, (F) CD40-D84/A, (G) CD40-N86/A, (H) CD40-S113/A, and (I) CD40-E114/A. In all cases the radiolabeled ([^{35}S]Met and [^{35}S]Cys) protein in the COS cell supernatants was purified with immobilized protein A and analyzed under reducing conditions.

side-chain characteristics, are possible receptor–ligand contacts. Residues were considered to be particularly attractive candidates if they spatially corresponded to residues in TNF-β involved in complex formation as reported by Banner et al. (1993). The purpose of initially focusing on the gp39 model rather than on the linkage map of the TNF-β/TNFR system in choosing residues to be targeted for substitution was to avoid "bias". If the contact map of TNF-β/TNFR alone was used as the selection criterion, no positions critical for receptor–ligand binding unique to gp39–CD40 could be identified.

CD40 Point Mutants. Using the criteria outlined above, we identified seven residues (R73, H76, Y82, D84, N86, S113, and E114) in the extracellular domain of CD40 which may be involved in gp39–CD40 binding (Figure 1A). All of these residues are contained within the TNFR homologous domains 2 and 3 of CD40. Each of these residues was individually replaced by an alanine using a PCR-based approach (Ho et al., 1989). PCR products encoding each of the CD40 mutants were completely sequenced to verify that the desired base substitutions had taken place and to detect potential secondary mutations introduced by the PCR experiment.

To facilitate the binding studies between the CD40 mutants and gp39, chimeric genes encoding the CD40-Ig fusion protein corresponding to each mutant were prepared as previously described (Hollenbaugh et al., 1992). The wild-type and mutant CD40-Ig fusion proteins were prepared by transient expression in COS cells and purified by affinity chromatography using a protein A column (Aruffo et al., 1990). All mutant DNAs directed the secretion of the appropriate fusion protein (Figure 2). However, mutant CD40-H76/A was a poor producer. Anti-CD40 and anti-human Ig binding studies with fixed and permeabilized COS cells transfected with a plasmid encoding CD40-H76 /A showed that this fusion protein was efficiently synthesized (data not shown). These data along with the results shown in Figure 2 suggest that the failure to detect high levels of CD40-H76/A is not due to lack of expression from the plasmid. No further work was carried out with this mutant.

To indirectly examine the structural integrity of the CD40 mutants and the role of the targeted residues on gp39 binding,

```
(A)
      62                    *     *           *   *   *   88
CD40: C G E S E F L D T W N R E T H C H Q H K Y C D P N L G
TNFR: C E S G S F T A S E N H L R H C L S C S K C R K E M G
      55                                                  81
                                                          *
                                    (104)                 * 114
CD40: L R V Q Q K G T S E T D T I C T C E E G - W H C T S E
TNFR: Q V E I S S C T V D R D T V C G C R K N Q Y R H Y W S
                                                          108

                                                          140
CD40: A C E S - C V L H R S C S P G F G V K Q I A T G V S D
TNFR: E N L F Q C F N C S L C L N G - T V H L S C Q E K Q N
                                                          134

            144
CD40: T I C E
TNFR: T V C T
            138

(B)
      125   * *   *       *               *   *           151
gp39: H V I S E A S S K T T S V L Q W A E K G Y Y T M S N N
TNFß: H L I G D P S - K Q N S - L L W R A N T D R A F L Q D
      32                                                  56

                                                          178
gp39: L V T L E N G K Q L T V K R Q G L Y Y I Y A Q V T F C
TNFß: G F S L S N - N S L L V P T S G I Y F V Y S Q V V F S
                                                          82

      *                                                   200
gp39: S N R E A - - - - S S Q A P F I A S L C L K S P - G R
TNFß: G K A Y S P K A T S S P L Y L A H E V Q L F S S Q Y P
                                                          109

      * *                                                 226
gp39: F E R I L L R A A N T H S S - A K P C G Q Q S I H L G
TNFß: F H V P L L S S Q K M V Y P G L Q E P W L H S M Y H G
                                                          136

                                  *     *                 253
gp39: G V F E L Q P G A S V F V N V T D P S Q V S H G T G F
TNFß: A A F Q L T Q G D Q L S T H T D G I P H L V L S P S T
                                                          163
```

FIGURE 1: CD40/TNFR and gp39/TNF-β structure-based sequence alignment. (A) Structure-based sequence alignment of the extracellular domain of CD40 versus the extracellular domain of the 55-kDa form of TNFR. (B) Structure-based sequence alignment of the extracellular domain of gp39 versus the extracellular domain of TNF-β. Residues targeted for replacement are shown (•). Conserved residues are shown in bold. Sequence homologies for the regions included in the CD40/TNFR alignment and the gp39/TNF-β alignment are approximately 26% and 25%, respectively.

structure. These residues include those involved in the formation of disulfide bonds and residues within the core regions of this molecule. Many of these TNFR residues were found to be conserved or conservatively replaced in CD40. These observations provide further evidence of the structural similarity between CD40 and TNFR, which is reflected in the assignment of corresponding (or topologically equivalent) residue positions in the sequence–structure alignment. Banner et al. (1993), who determined the crystal structure of the TNF-β/TNFR complex, generated a linkage diagram of the TNF-β/TNFR contacts by calculating the reduction of the solvent-accessible surface of the two proteins upon complex formation. In the absence of a three-dimensional model of CD40, this structure-oriented alignment was combined with the TNF-β/TNFR linkage map to select CD40 residues for mutagenesis.

A similar approach was used in the generation of a structure-based alignment of gp39 with TNF-β (Figure 1B). This alignment, in conjunction with analysis of our previously reported three-dimensional model of the gp39 homotrimer (Aruffo et al., 1993; Bajorath et al., 1993), allowed the identification of a number of gp39 residues predicted to be topologically equivalent to solvent-accessible residues in the TNF-β X-ray structure, which, due to their location and

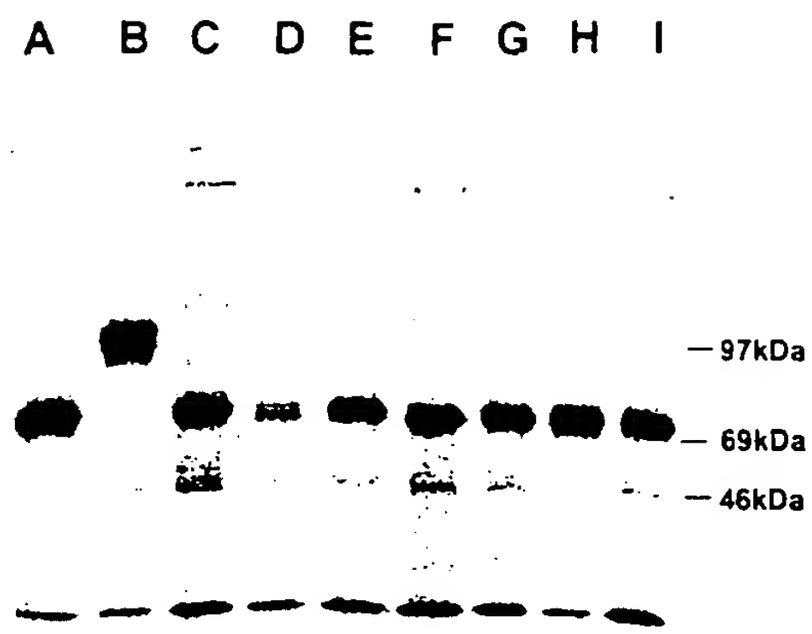

FIGURE 2: Wild-type and mutant CD40-Ig proteins. SDS–PAGE analysis of wild-type and mutant proteins obtained from the supernatant of COS cell transfectants: (A) wild-type CD40-Ig, (B) control fusion protein Leu 8-Ig, (C) CD40-R73/A, (D) CD40-H76/A, (E) CD40-Y82/A, (F) CD40-D84/A, (G) CD40-N86/A, (H) CD40-S113/A, and (I) CD40-E114/A. In all cases the radiolabeled ([^{35}S]Met and [^{35}S]Cys) protein in the COS cell supernatants was purified with immobilized protein A and analyzed under reducing conditions.

side-chain characteristics, are possible receptor–ligand contacts. Residues were considered to be particularly attractive candidates if they spatially corresponded to residues in TNF-β involved in complex formation as reported by Banner et al. (1993). The purpose of initially focusing on the gp39 model rather than on the linkage map of the TNF-β/TNFR system in choosing residues to be targeted for substitution was to avoid "bias". If the contact map of TNF-β/TNFR alone was used as the selection criterion, no positions critical for receptor–ligand binding unique to gp39–CD40 could be identified.

CD40 Point Mutants. Using the criteria outlined above, we identified seven residues (R73, H76, Y82, D84, N86, S113, and E114) in the extracellular domain of CD40 which may be involved in gp39–CD40 binding (Figure 1A). All of these residues are contained within the TNFR homologous domains 2 and 3 of CD40. Each of these residues was individually replaced by an alanine using a PCR-based approach (Ho et al., 1989). PCR products encoding each of the CD40 mutants were completely sequenced to verify that the desired base substitutions had taken place and to detect potential secondary mutations introduced by the PCR experiment.

To facilitate the binding studies between the CD40 mutants and gp39, chimeric genes encoding the CD40-Ig fusion protein corresponding to each mutant were prepared as previously described (Hollenbaugh et al., 1992). The wild-type and mutant CD40-Ig fusion proteins were prepared by transient expression in COS cells and purified by affinity chromatography using a protein A column (Aruffo et al., 1990). All mutant DNAs directed the secretion of the appropriate fusion protein (Figure 2). However, mutant CD40-H76/A was a poor producer. Anti-CD40 and anti-human Ig binding studies with fixed and permeabilized COS cells transfected with a plasmid encoding CD40-H76 /A showed that this fusion protein was efficiently synthesized (data not shown). These data along with the results shown in Figure 2 suggest that the failure to detect high levels of CD40-H76/A is not due to lack of expression from the plasmid. No further work was carried out with this mutant.

To indirectly examine the structural integrity of the CD40 mutants and the role of the targeted residues on gp39 binding,

Table 1: Binding of Anti-CD40 mAbs to CD40 Mutants[a]

	Leu 8	CD40 wt	S113/A	D84/A	N86/A	R73/A	Y82/A	E114/A	Western blot
40−1.87	−	+++	+++	+++	+++	+++	+++	+	−
40−2.210	−	+++	+++	+++	+++	−	+++	+++	−
40−2.131	−	+++	++	+	+++	++	−	+++	+
40−1.62	−	+++	++	++	+++	+++	+++	+++	+
G28−5	−	+++	+++	+++	+++	+++	+++	+++	+

[a] Equal amounts of wild-type and mutant CD40-Ig fusion proteins were immobilized in the wells of a 96-well plastic dish, and the binding of anti-CD40 mAbs was monitored by ELISA. Strong binding (+++) was based on antibody binding to wild-type CD40-Ig. Background levels of binding (−) were based on antibody binding to Leu 8-Ig, an unrelated fusion protein. The ability of each anti-CD40 mAb to recognize wild-type CD40-Ig blotted onto a nylon membrane is shown (Western blot).

we first assessed the reactivity of each mutant with a panel of five different anti-CD40 mAbs (Table 1). Antibodies 40−1.87 and 40−2.210 do not blot CD40 and presumably recognize discontinuous or conformational epitopes; antibodies 40−1.62, 40−2.131, and G28-5 blot CD40 and presumably recognize linear epitopes (Table 1). Antibody 40−1.62 strongly blocks gp39 binding, while antibodies 40−1.87, 40−2.131, 40−2.210, and G28-5 weakly block gp39 binding (A. W. Siadak and M. Gordon, unpublished). These results suggest that these antibodies recognize at least three distinct CD40 epitopes. As shown in Table 1, all of these antibodies bound to wild-type CD40 and the CD40 mutants, with two exceptions. Antibody 40−2.210 did not bind CD40-R73/A and antibody 40−2.131 did not bind CD40-Y82/A. Also, antibody 40−1.87 bound weakly to CD40-E114/A and antibody 40−2.131 bound weakly to CD40-D84/A.

gp39 Point Mutants. On the basis of the criteria outlined above, we identified nine gp39 residues predicted to be solvent-accessible (S131, T135, K143, Y145, N180, F201, E202, N240, and D243) as targets for mutagenesis. These nine residues were replaced by alanine, either individually (K143, Y145, and N180) or as double mutants. Three double mutants were prepared in which residue pairs S131 and T135, F201 and E202, and N240 and D243 were changed to alanine (Figure 1B). The residues in each double mutant are predicted to be proximal to each other on the gp39 protein surface (Figure 10). The gp39 mutants were prepared using a PCR-based approach (Ho et al., 1989). Each mutant cDNA was fully sequenced to ensure that it encoded the desired mutant protein and to verify that no secondary mutations had been introduced during the PCR experiment.

To facilitate the binding studies between the gp39 mutants and CD40, chimeric genes encoding soluble forms of the mutant gp39 (sgp39) proteins were prepared. These recombinant genes consist of a cDNA fragment encoding the extracellular domain of murine CD8 fused onto a cDNA fragment encoding the extracellular domain of gp39 (Hollenbaugh et al., 1992). The wild-type and mutant sgp39 fusion proteins were produced by transient expression in COS cells (Hollenbaugh et al., 1992). As shown in Figure 3 the mutants were secreted by the transfected COS cells. The gp39−N240/A-D243/A mutant was poorly secreted, despite efficient synthesis as demonstrated by anti-murine CD8 and anti-gp39 mAb binding of transfected COS cells. No further work was attempted with this mutant.

To indirectly examine the structural integrity of these gp39 mutants, we examined their reactivity with a panel of five different anti-gp39 mAbs (Table 2). All of these antibodies block gp39 binding to CD40 (A. W. Siadak, M. Gordon, and J. S. Marken, unpublished) and did not blot the gp39 antigen, suggesting that they recognize nonlinear or conformational epitopes on gp39 (Table 2). All of the anti-gp39

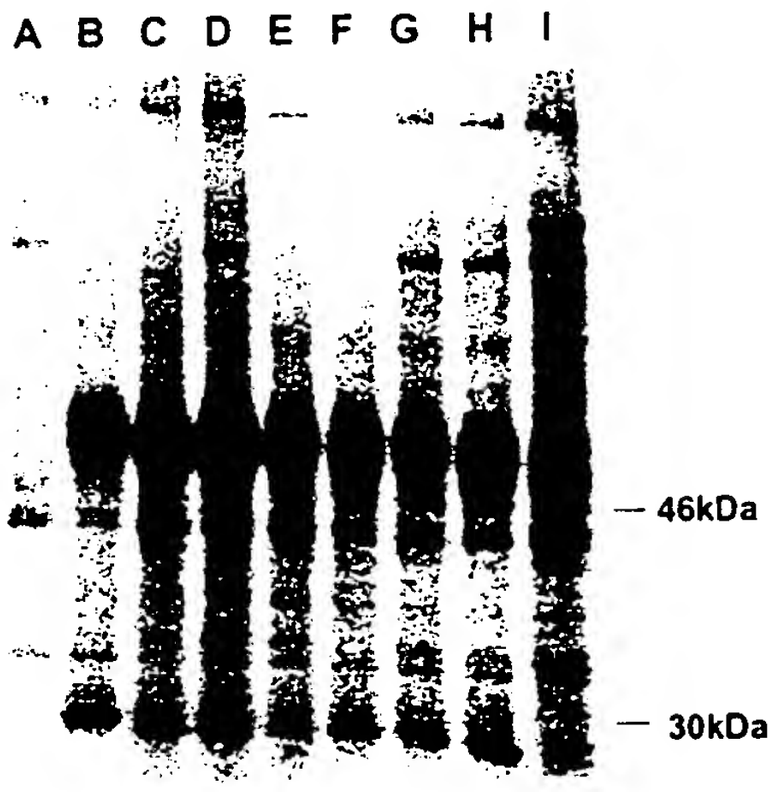

FIGURE 3: Wild-type and mutant sgp39 proteins. SDS−PAGE analysis of wild-type and mutant proteins obtained from the supernatant of COS cell transfectants: (A) mock transfected COS cells, (B) wild-type gp39, (C) gp39−E129/A, (D) gp39−S131/A-T135/A, (E) gp39−K143/A, (F) gp39−Y145/A, (G) gp39−N180/A, (H) gp39−F201/A-E202/A, and (I) gp39N240/A-D243/A. In all cases the radiolabeled ([^{35}S]Met and [^{35}S]Cys) protein in the COS cell supernatants was immunoprecipitated with the anti-murine CD8 mAb G53-6, followed by hamster anti-rat Ig coupled to Sepharose and analyzed under reducing conditions.

mAbs tested bound to the wild-type and mutant gp39, with one exception: mAb 39−1.26 did not recognize gp39−K143/A (Table 2). Two of the mutants showed reduced binding to a subset of antibodies. gp39−S131/A-T135/A bound weakly to mAb 39−1.59, and gp39K143/A bound weakly to both mAbs 39−1.124 and 39−1.156 (Table 2).

The possibility that mutations in the gp39 domain of the chimeric protein affect the structure of the CD8 domain is unlikely. The CD8 fragment has been used as a tag polypeptide for the construction of a number of different soluble type II membrane proteins, and regardless of the fusion partner used no changes in the anti-CD8 antibody recognition have been observed (Aruffo et al., 1993; Hollenbaugh et al., 1992).

Binding of CD40 Mutants to gp39. To determine the contribution of each mutated CD40 residue to gp39 binding, three different binding assays were used. In the first assay the ability of wild-type and mutant CD40-Igs, in solution, to bind to a Jurkat cell line variant which constitutively expresses low levels of gp39 (BMS-10 cells) was examined by flow cytometry (Figure 4). In this assay CD40-Ig mutants CD40-Y82/A and CD40-D84/A showed no binding to BMS-10 cells, mutants CD40-N86/A and CD40-S113/A showed significantly diminished binding, while mutants CD40-R73/A and CD40-E114/A had slightly diminished binding to gp39. A control immunoglobulin fusion protein, Leu 8-Ig (Walz et al., 1990) did not bind to BMS-10 cells.

Table 2: Binding of Anti-gp39 mAbs to gp39 Mutants[a]

	CD72	gp39	E129/A	S131/A-T135/A	K143/A	Y145/A	N180/A	N246/A-D133/A	E129/G	S128/R	Western blot
39−1.26	−	+++	+++	+++	−	+++	+++	+++	+	−	−
39−1.59	−	+++	−	+	+++	+++	+++	+++	−	−	−
39−1.124	−	+++	++	+++	+	+++	+++	+++	+	−	−
39−1.156	−	+++	++	+++	+	+++	+++	+++	+	−	−
39−7.3	−	+++	+++	+++	+++	+++	+++	+++	++	−	−

[a] Equal amounts of wild-type and mutant sgp39 were immobilized in the wells of a 96-well plastic dish, and the binding of anti-gp39 mAbs was monitored by ELISA. The levels of captured sgp39 proteins immobilized in the wells were normalized as described in the Materials and Methods section. Strong binding (+++) was based on antibody binding to wild-type sgp39. Background levels of binding (−) were based on antibody binding to sCD72. The ability of each anti-gp39 mAb to recognize wild-type sgp39 blotted onto a nylon membrane is shown (Western blot).

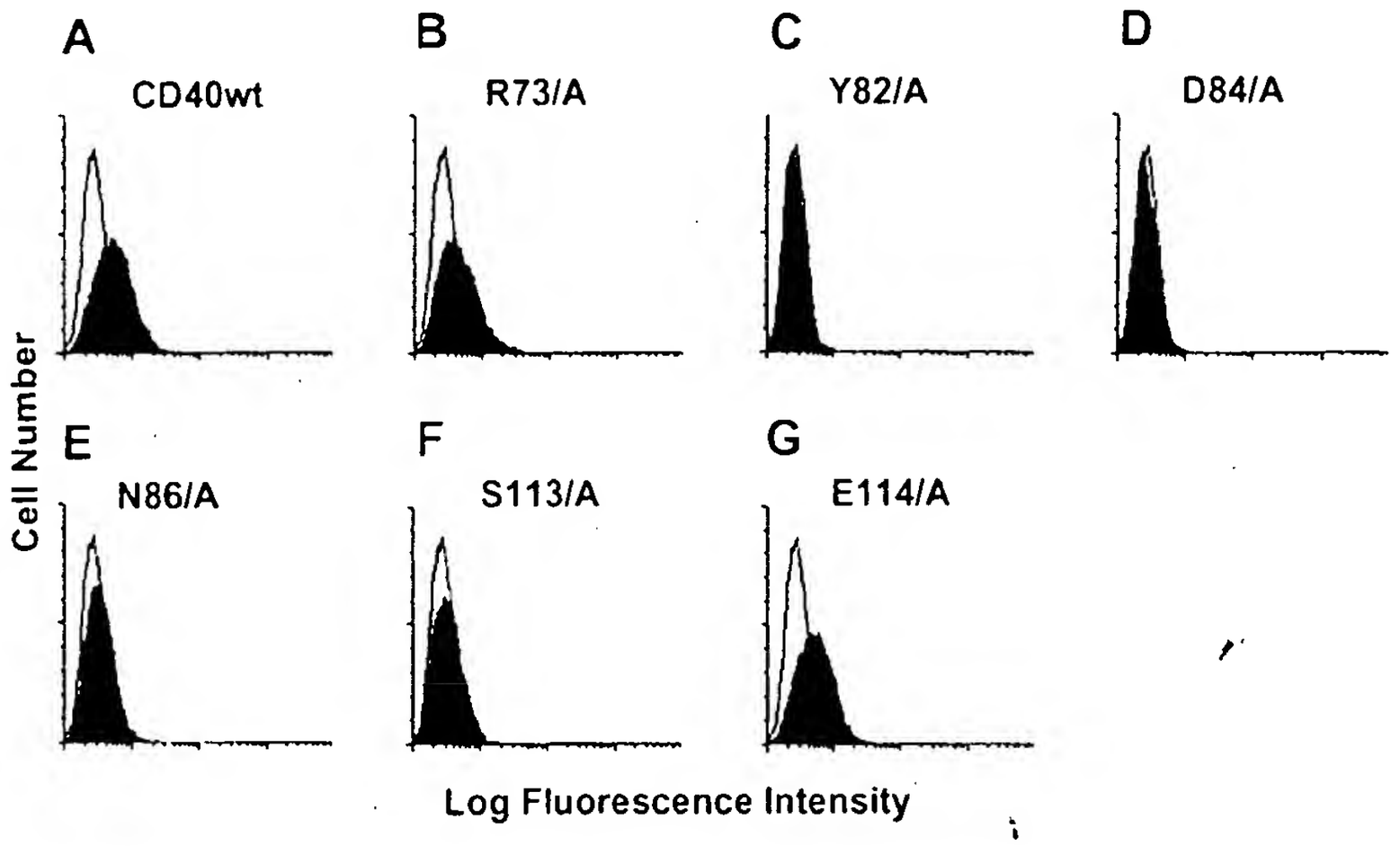

FIGURE 4: Binding of wild-type and mutant CD40-Ig to cells expressing gp39. Flow cytometry profiles of wild-type CD40-Ig and mutant CD40-Ig fusion proteins (filled in profiles) binding to BMS-10 cells. The binding of the control fusion protein Leu 8-Ig (MFI = 2.85) to the same cell line is included as a comparison in each binding experiment (empty profile). Panels: (A) CD40-Ig wild-type (MFI = 6), (B) CD40-R73/A (MFI = 6), (C) CD40-Y82/A (MFI = 3), (D) CD40-D84/A (MFI = 3), (E) CD40-N86/A (MFI = 4), (F) CD40-S113/A (MFI = 4), and (G) CD40-E114/A (MFI = 5).

In the second assay, wild-type sgp39 was immobilized on plastic plates which had been precoated with an anti-murine CD8 mAb (Hollenbaugh et al., 1992). The binding of wild-type and mutant CD40-Igs to the immobilized gp39 was examined by ELISA using an HRP-conjugated anti-human IgG mAb (Figure 5). We obtained results similar to those observed in the previous binding assay. CD40-Ig mutants CD40-Y82/A and CD40-D84/A did not bind sgp39 while CD40-N86/A recognized sgp39 very poorly. Mutants CD40-R73/A and CD40-S113/A had reduced but measurable binding to sgp39, while mutant CD40-E114/A bound sgp39 like wild-type CD40-Ig. As expected, a control immunoglobulin chimeric protein, Leu 8-Ig (Walz et al., 1990), did not bind sgp39.

In the third assay, wild-type and mutant CD40-Igs were immobilized on plastic plates precoated with anti-human IgG antibody, and their ability to bind BMS-10 cells was examined. This cell adhesion assay provides for a high avidity interaction between the receptor (CD40 immobilized on plastic) and its ligand (gp39 on the cell surface) by maximizing the number of receptor−ligand interactions (Hollenbaugh et al., 1993). As shown in Figure 6, mutants CD40-R73/A, CD40-S113/A, CD40-E114/A, and wild-type CD40-Ig bound comparably to the BMS-10 cells, while mutants CD40-Y82/A, CD40-D84/A, and CD40-N86/A bound very poorly, if at all, to these same cells. The control fusion protein Leu 8-Ig did not bind to the BMS-10 cells (Figure 6).

Binding of gp39 Mutants to CD40. The binding of wild-type and mutant gp39 to CD40 was assessed using two assays. In the first assay Daudi cells, which express CD40, were incubated with COS cell supernatants containing either wild-type or mutant sgp39. The binding of the sgp39 was assayed by flow cytometry (Figure 7). Two sgp39 mutants showed reduced binding to the Daudi cells, gp39−K143/A and gp39−Y145/A. The other sgp39 mutants and wild-type sgp39 had binding comparable to that of Daudi cells. A control fusion protein, sCD72 (Hollenbaugh et al., 1992), did not bind to the Daudi cells.

In the second binding assay, wild-type and mutant sgp39 were immobilized on plastic plates which had been precoated with an anti-murine CD8 mAb. The levels of captured wild-type and mutant sgp39 were normalized with the aid of a second anti-murine CD8 mAb as described in the Materials and Methods section. The binding of CD40-Ig to the immobilized sgp39 was monitored by ELISA. As in the previous assay, we observed that gp39−K143/A and gp39−Y145/A bound CD40-Ig poorly (Figure 8). As expected, a control fusion protein, sCD72 (Hollenbaugh et al., 1992), did not bind to CD40-Ig.

X-HIM-Derived gp39 Mutants Binding to CD40. We examined the location of the naturally occurring amino acid substitutions found in the gp39 obtained from patients with X-HIM. Deletion mutants were not considered in this analysis as they can be expected to lead to structural perturbations of the protein. The location of the following

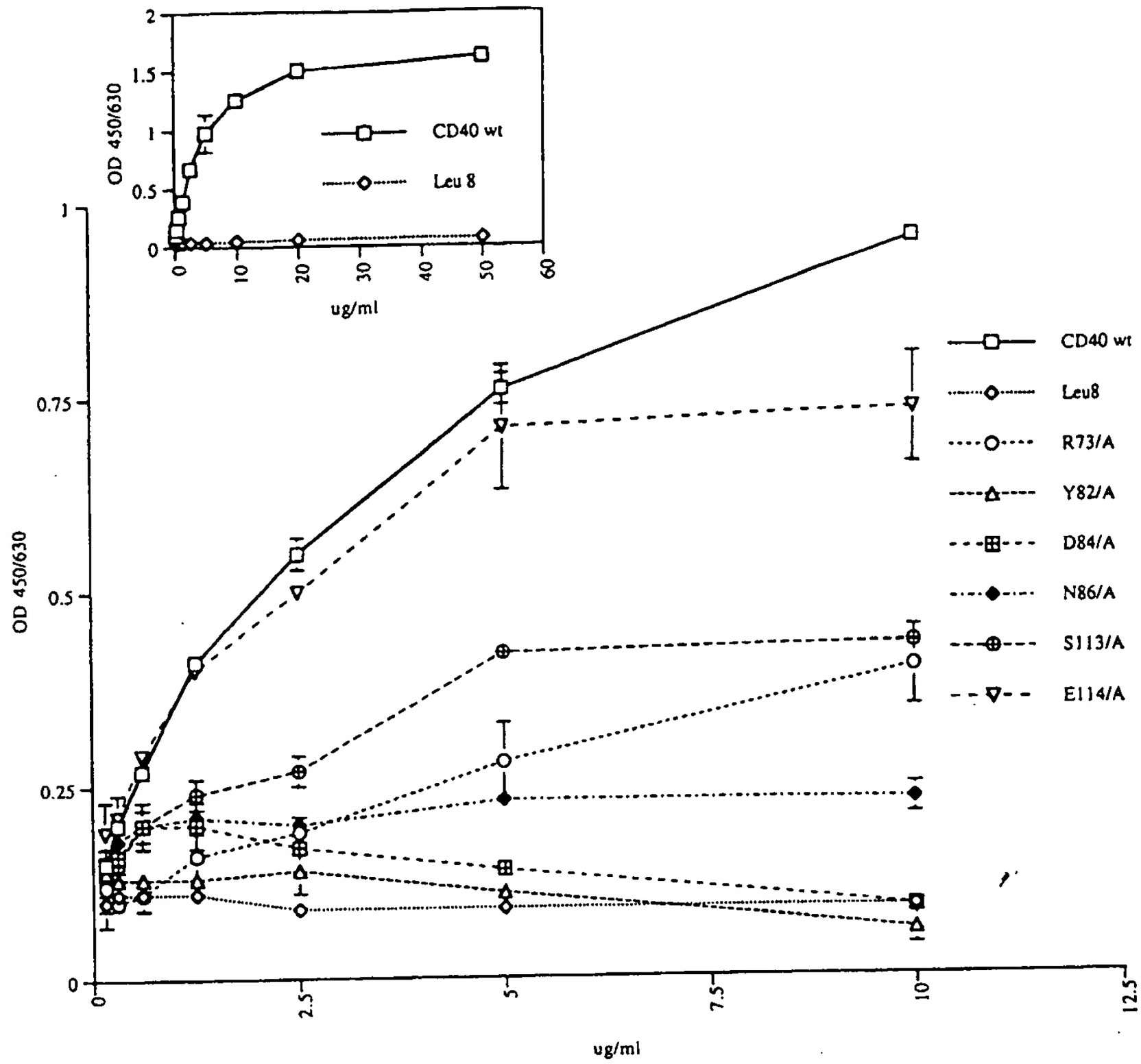

FIGURE 5: Binding of wild-type and mutant CD40-Igs to sgp39. Soluble recombinant gp39 was immobilized on plastic as described in the Materials and Methods section, and the binding of increasing concentrations of wild-type or mutant CD40-Ig fusion proteins was monitored by ELISA. Bars indicate the standard error of the mean of triplicate analysis. Bars indicate the standard error of the mean of duplicate analysis.

naturally occurring gp39 point mutations was examined: A123/E, the double mutant S128/R-E129/G, W140/G, L155/P, T211/D, G227/V, L231/S, A235/P and T254/M (Villa et al., 1994; Aruffo et al., 1994; Ochs & Aruffo, 1993; Callard et al., 1993; and D. Hollenbaugh, and H. D. Ochs, unpublished). All the mutations affect residues which are either buried within a gp39 monomer or at the gp39 trimer interface, with two exceptions, residues L155 and E129. Residue L155/P is partially surface-accessible, but its side chain is predicted to participate in a hydrophobic packing arrangement involving the buried β-sheet framework residues V126 and L161. For this reason, L155 is considered to be structurally important and not accessible as a putative CD40 contact residue. The only naturally occurring gp39 mutant identified to date which potentially affects the CD40/gp39 interactions directly is E129/G, found in the double mutant S128/R-E129/G.

To examine if the lack of CD40 binding by this natural gp39 double mutant was caused by both or only one of these substitutions and to determine the contribution of each of these residues to the formation of the gp39–CD40 complex, two additional gp39 mutants were prepared, gp39–S128/R and gp39–E129/G. The binding of these two mutants to CD40 was examined using the two binding assays described above.

As shown in Figure 9A, mutant gp39–S128/R did not bind Daudi cells, while mutant gp39–E129/G had reduced but detectable binding. Using the binding assay in which the wild-type and mutant sgp39 proteins are immobilized on plastic plates precoated with an anti-murine CD8 mAb and CD40-Ig binding is monitored by ELISA, we found that gp39–E129/G bound CD40-Ig poorly while the binding of gp39–S128/R was close to background levels (Figure 9B). We examined the ability of these sgp39 point mutants to bind to our panel of five anti-gp39 mAbs. The mutant gp39–E129/G was recognized, albeit weakly, by all the antibodies with the exception of mAb 39–1.59, while mutant gp39–S128/R was recognized by none of the mAbs (Table 2).

Since the naturally occurring mutation of E129 to glycine resulted in reduced but detectable binding to gp39, we speculated that this mutation may increase the flexibility of this region of gp39, thereby interfering with CD40 binding. We therefore prepared an additional mutant at this position by changing E129 to alanine (gp39-E129/A, Figure 3). This mutant probes the side-chain contribution of E129 to CD40 binding without introducing increased flexibility. In contrast to gp39–E129/G, gp39–E129/A bound CD40 like wild-type in our two binding assays (Figures 7 and 8). When we examined the binding of gp39–E129/A to our panel of anti-gp39 mAbs, we found that it bound to all the antibodies, with one exception, mAb 39–1.59 (Table 2).

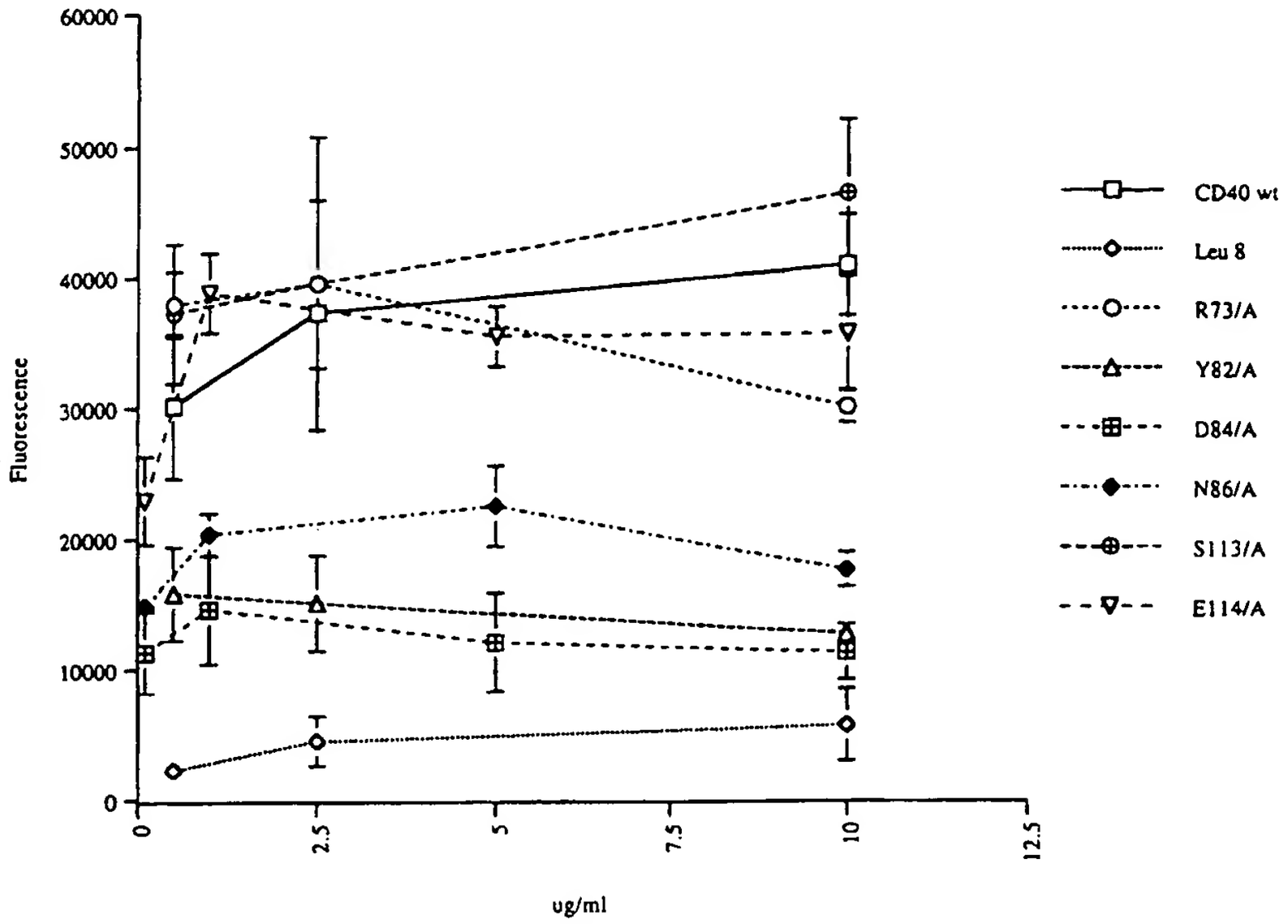

FIGURE 6: Binding of immobilized wild-type and mutant CD40-Ig to cells expressing gp39. Increasing concentrations of wild-type and mutant CD40-Ig or the control fusion protein Leu 8-Ig were immobilized on plastic as described in the Materials and Methods section. The binding of fluorescein-labeled BMS-10 cells to the immobilized proteins was then monitored. Bars indicate the standard error of the mean of triplicate analysis.

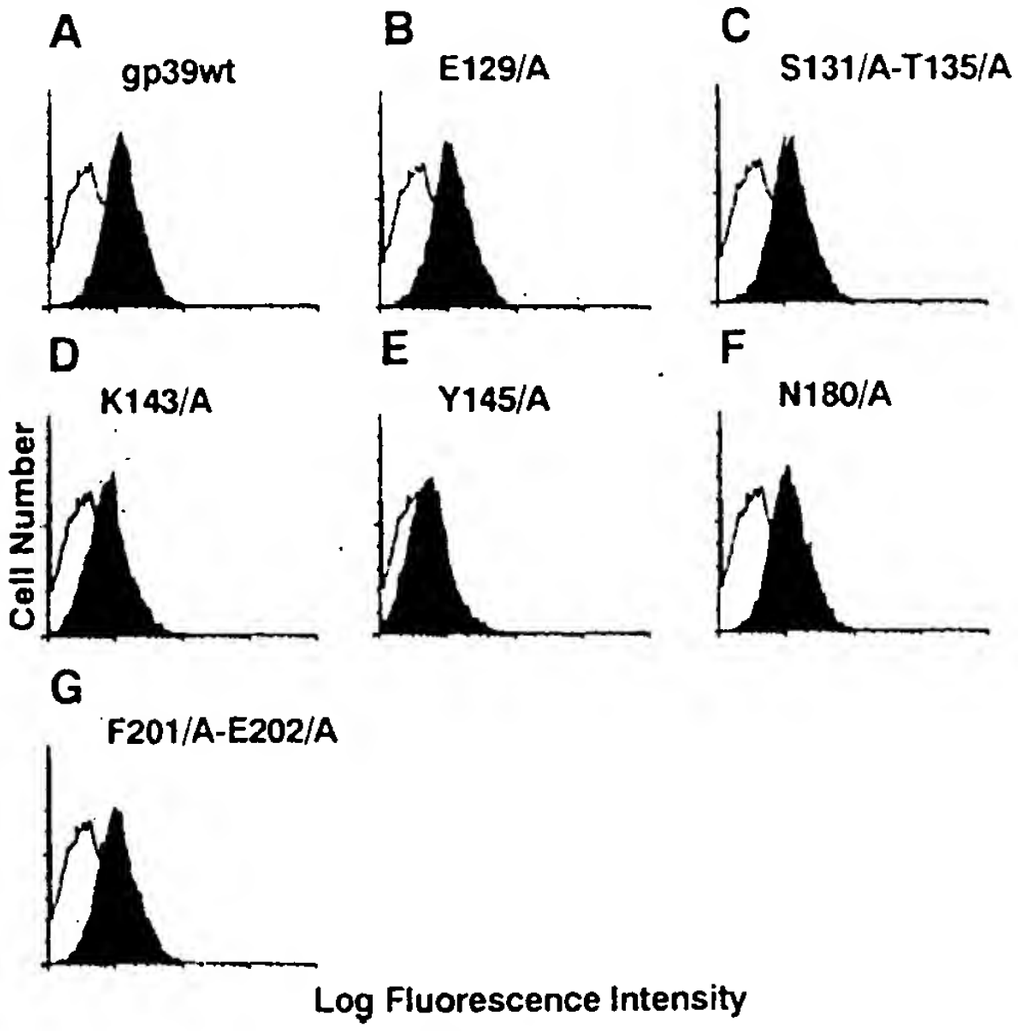

FIGURE 7: Binding of wild-type and mutant sgp39 to cells expressing CD40. Flow cytometry profiles of wild-type and mutant sgp39 fusion proteins (filled in profiles) binding to Daudi cells. The binding of the control fusion protein sCD72 (MFI = 4) to the same cell line is included as a comparison in each binding experiment (empty profile). Panels: (A) sgp39 wild-type (MFI = 15) , (B) gp39−E129/A (MFI = 14), (C) gp39−S131/A-T135/A (MFI = 16), (D) gp39−K143/A (MFI = 10), (E) gp39−Y145/A (MFI = 7), (F) gp39−N180/A (MFI = 14), and (G) gp39−N246/A-D133/A (MFI = 14).

DISCUSSION

The studies presented herein have shown that CD40 residues Y82, D84, and N86 are critical for gp39 binding. The mutants CD40-Y82/A, -D84/A, and -N86/A bound gp39 very weakly in three different binding assays, including a high-avidity cell adhesion assay in which the binding of wild-type or mutant CD40-Ig immobilized on plastic to a cell line which constitutively expresses gp39 (BMS-10 cells) was examined. These studies also showed that CD40 residues R73, E114, and S113 are not critical for gp39 binding. The CD40-E114/A binding was comparable to wild-type in two of three assays used and only slightly reduced in the third assay. However, the CD40-R73/A and CD40-S113/A mutants showed reduced binding relative to wild-type in two of the three binding assays used. One assay examined the binding of wild-type and mutant CD40-Ig to BMS-10 by flow cytometry; the second assay examined the binding of these proteins to sgp39 immobilized on plastic. In the third assay system, the high-avidity cell adhesion assay, both CD40-R73/A and CD40-S113/A bound gp39 as well as wild-type. These results suggest that, although not critical for gp39 binding, CD40 residues R73 and S113 may contribute to the gp39−CD40 interaction.

Table 3 summarizes the mutagenesis data reported in this study. In the absence of crystallographic data, we cannot rule out the possibility that the structural integrity of the CD40 or gp39 mutants has been compromised. However, the ability of the CD40 mutants to bind a panel of five anti-CD40 mAbs, which recognize at least three distinct conformation-dependent CD40 epitopes, suggests that the mutants are structurally sound. Two point mutants were no longer recognized by one of the mAbs. Mutant CD40-R73/A was not recognized by mAb CD40−2.210 while CD40-Y82/A was not recognized by mAb 40−2.131. These results suggest that these two point mutants are part of the epitope recognized by these antibodies. The observation that CD40-Y82/A no longer binds gp39 and mAb 40−2.131 suggests that the gp39 binding site and the epitope recognized by this mAb are overlapping. Equivalent observations were made for the gp39 mutants (see below)

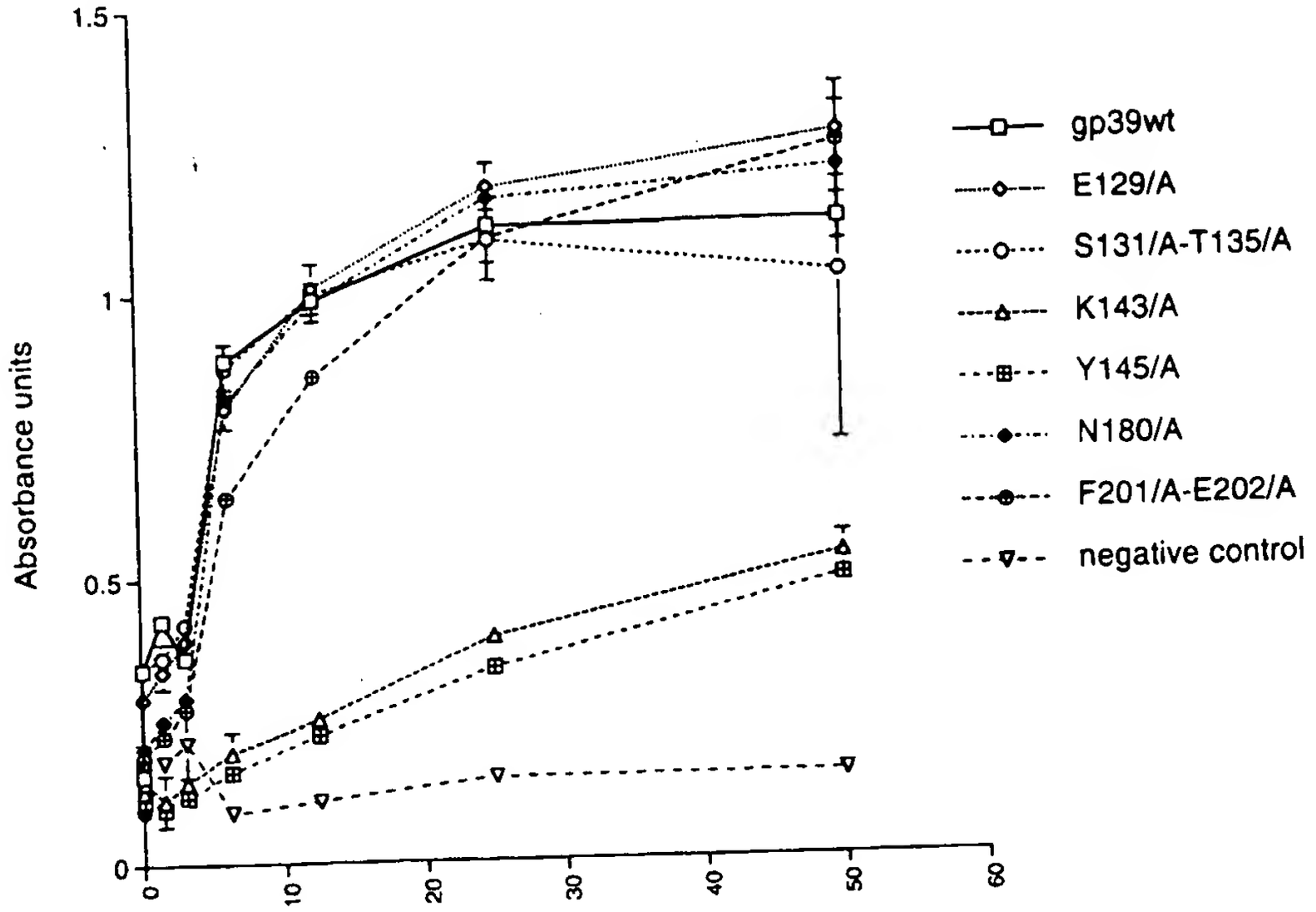

FIGURE 8: Binding of wild-type and mutant sgp39 to CD40-Ig. Wild-type or mutant sgp39 was immobilized on plastic as described in the Materials and Methods section, and the binding of increasing concentrations of CD40-Ig fusion proteins was monitored by ELISA.

Binding assays with gp39 mutants resulted in the identification of two residues which are critical for the gp39–CD40 interaction. The gp39 mutants gp39-K143/A and -Y145/A have significantly reduced binding to CD40. Two different binding assays were used in these studies; one examined the binding of wild-type and mutant sgp39 mutants to a B cell line expressing CD40 by flow cytometry; the second examined the binding of CD40-Ig to wild-type and mutant sgp39 immobilized on plastic. Both assays gave similar results. As in the case of the CD40 mutants, we indirectly examined the structural integrity of the gp39 mutants by examining their ability to bind to a panel of five anti-gp39 mAbs. Three gp39 point mutants failed to bind to two different antibodies: gp39–E129/A and gp39–E129/G failed to bind mAb 39–1.59 and gp39–K143/A was not recognized by mAb 39–1.26. All the antibodies in this panel are able to block gp39 binding to CD40 but are unable to blot gp39 (A. W. Siadak, M. Gordon, and D. Hollenbaugh, unpublished). These results suggest that these five mAbs recognize at least three distinct gp39 epitopes.

The predicted location of CD40 and gp39 mutations which affect receptor–ligand interactions can be analyzed using the structural information available from the TNF-β/TNFR complex (Banner et al., 1993). The reported analysis of the TNF-β/TNFR complex identified surface residues that become solvent-inaccessible on complex formation and therefore form the receptor–ligand interface (Banner et al., 1993). However, residues involved in the formation of a protein–protein interface may not contribute equally to binding (Jin et al., 1992; Novotny et al., 1989). Thus, contact analysis does not necessarily parallel the results of mutagenesis experiments. In the case of CD40, all residues selected for mutagenesis correspond to TNFR residues that were buried upon TNF-β/TNFR complex formation. Mutation of five (R73, Y82, D84, N86, and S113) of the six selected residues resulted in reduced or absent binding, suggesting that these residues contribute substantially to gp39 binding. In the case of gp39, three of the nine selected residues (T135, E202, and D243) correspond to residues of TNF-β that are not involved in the TNF-β/TNFR interface while the six other residues selected (S131, K143, Y145, N180, F201, and N240) correspond to TNF-β residues that are at the TNF-β/TNFR interface. Only two of the residues selected, K143 and Y145, were found to be critical for the interaction with CD40. Both of these are located at the TNF-β/TNFR interface.

It is possible to compare the results of the mutagenesis experiments described here with the previously published mutagenesis studies on TNF-α and TNF-β. This was facilitated by the recent publication of a comprehensive review of mutagenesis studies on the TNF molecules (Van Ostade et al., 1994). The effect of TNF mutants was assessed using a cell-based cytotoxicity assay which provides an indirect measure of receptor binding to the TNF mutants. TNF-β residues corresponding to three of nine selected gp39 positions have been subjected to mutagenesis and cytotoxicity assays (gp39/TNF-β, K143/N48, Y145/D50, and N240/H150). Only mutation of one of these three positions, D50, results in inactive TNF-β molecules in cytotoxicity assays, while the mutants appear to be structurally intact (Van Ostade et al., 1994). D50 in TNF-β corresponds to Y145 in gp39, one of the two residues found to be involved in the interaction of gp39 with CD40. In contrast, mutations of residue N48 in TNF-β, which corresponds to K143, the second gp39 residue shown to be involved in the CD40 interaction, resulted in a TNF-β mutant which was fully active in cytotoxicity assays. These observations suggest the presence of both similarities and differences in the contribution of different surface residues in receptor–ligand binding in the TNF and TNFR family of receptor–ligand pairs.

Recently, various groups, including ours, have reported that defects in gp39 are the molecular basis for X-HIM

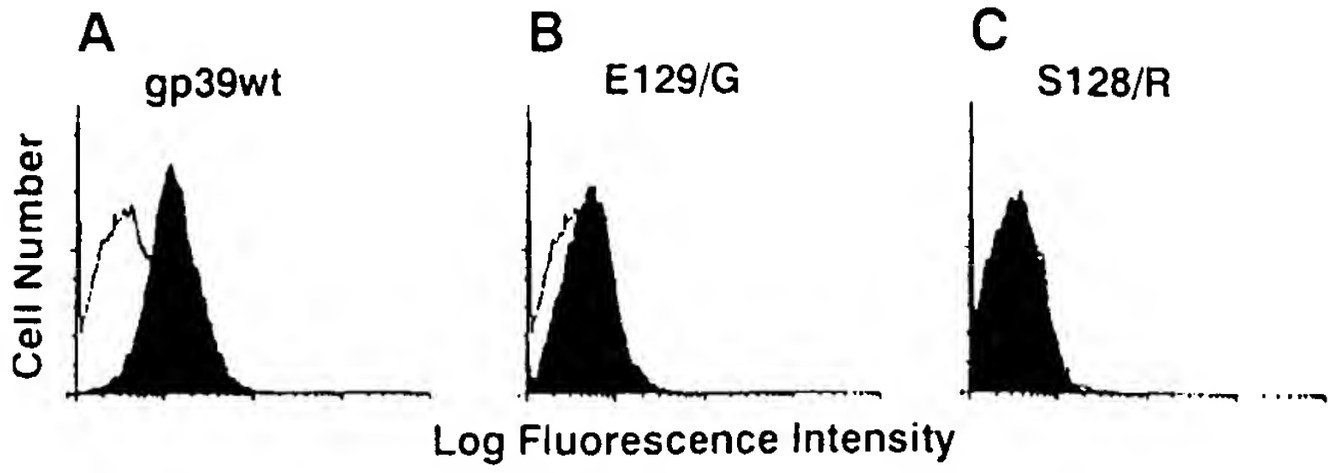

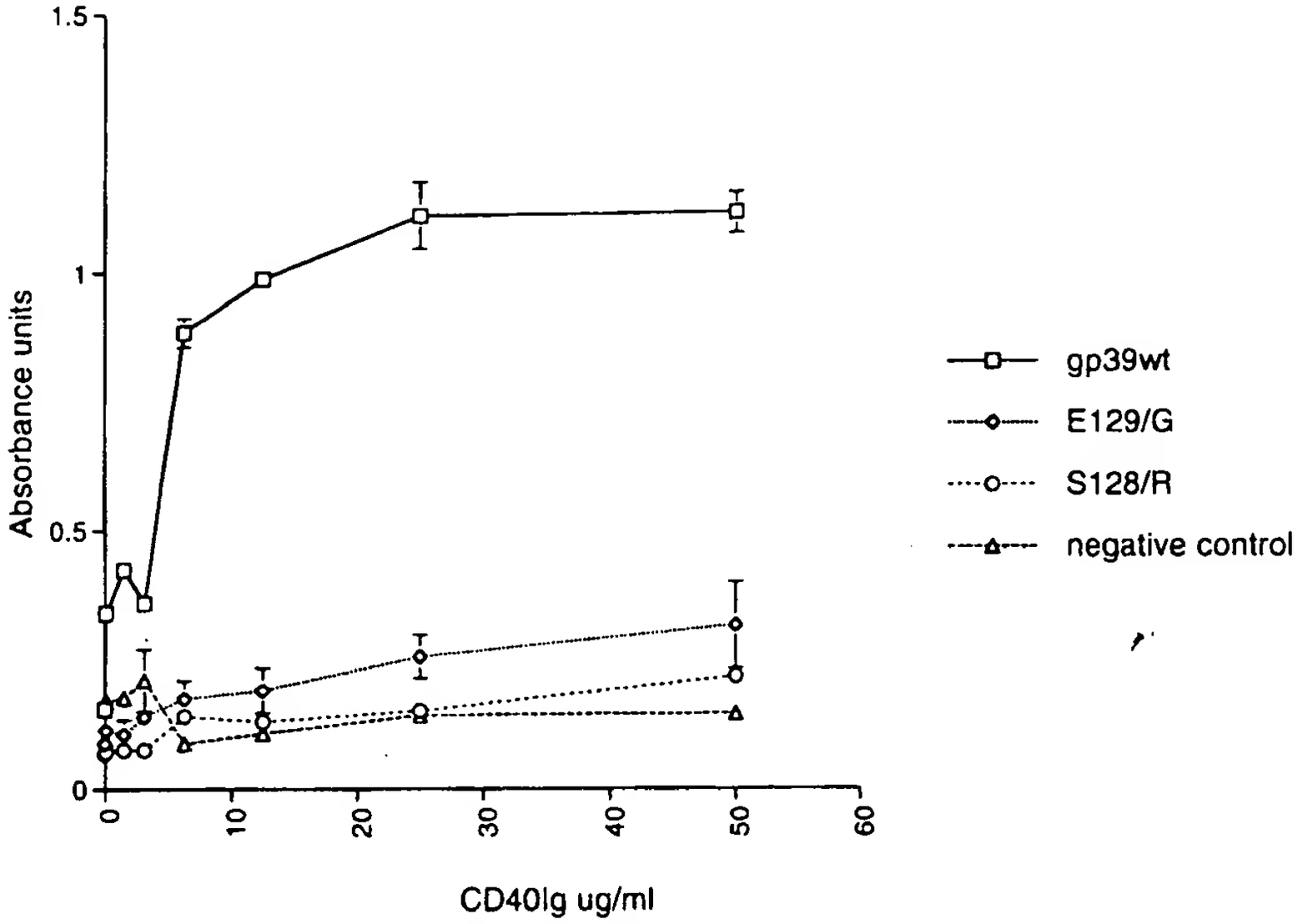

FIGURE 9: Binding studies with X-HIM-derived gp39 mutants. (A) Flow cytometry profiles of wild-type (gp39wt) and mutant sgp39 [E129/G (MFI = 6), S128/R (MFI = 4)] binding to CD40 expressing Daudi cells (filled in curves). The binding of the control fusion protein sCD72 (MFI = 4) to the same cell line is included as a comparison in each binding experiment (empty profile). (B) ELISA analysis of wild-type and mutant sgp39 (E129/G, S128/R), immobilized on plastic, binding to increasing concentrations of CD40-Ig. Bars indicate the standard error of the mean of duplicate analysis.

Table 3: Binding of CD40 Mutants[a]

	CD40wt	R73/A	H76/A	Y82/A	D84/A	N86/A	S113/A	E114/A
FACS	+++	++	N/A	−	−	+	+	++
ELISA	+++	++	N/A	−	−	+	++	+++
adhesion	+++	+++	N/A	+	+	+	+++	+++

	gp39wt	S128/R	E129/A	E129/G	S131/A	T135/A	K143/A	Y145/A	N180/A	F201/A	E202/A	N240/A	D243/A
FACS	+++	−	+++	+	+++	+++	+	+	+++	+++	+++	+++	+++
ELISA	+++	+	+++	+	+++	+++	+	+	+++	+++	+++	+++	+++

[a] The binding efficacies of all CD40 and gp39 mutants, compared to CD40 and gp39 wild-type, respectively, are summarized. FACS, ELISA, and adhesion data are included as given in the text.

(Aruffo et al., 1993; Allen et al., 1993; Korthauer et al., 1993; Di Santo et al., 1993; Fuleihan et al., 1993). We examined the location of all the amino acid substitutions encoded by the defective gp39 genes of X-HIM patients studied to date in an effort to identify gp39 mutants that lacked CD40 binding by virtue of having sustained changes in residues that are involved in direct receptor−ligand contacts. One patient was identified whose defective gene encodes a mutant gp39 protein with two amino acid substitutions, one of which, E129, would be predicted to be a solvent-accessible residue (Aruffo et al., 1993). We examined the contribution of each of these amino acid substitutions to CD40 binding by preparing two additional gp39 mutants, gp39−S128/R and gp39−E129/G. Using the two binding assays described above, we examined the interaction of these two gp39 mutants with CD40. We found that mutant gp39−E129/G showed significantly decreased binding to CD40 in both assays and mutant gp39−S128/R was unable to bind CD40 in both assays. E129 in gp39 corresponds to D36 in TNF-β; substitution of this residue with asparagine, histidine, or tyrosine did not affect TNF function. To examine if the effect of the E129/G mutation was due to increased flexibility in this region of the protein, resulting from the introduction of a glycine residue, or due to the absence of a specific side-chain molecular contact, mutant gp39−E129/A was prepared and tested for CD40 binding. This mutant bound CD40 like

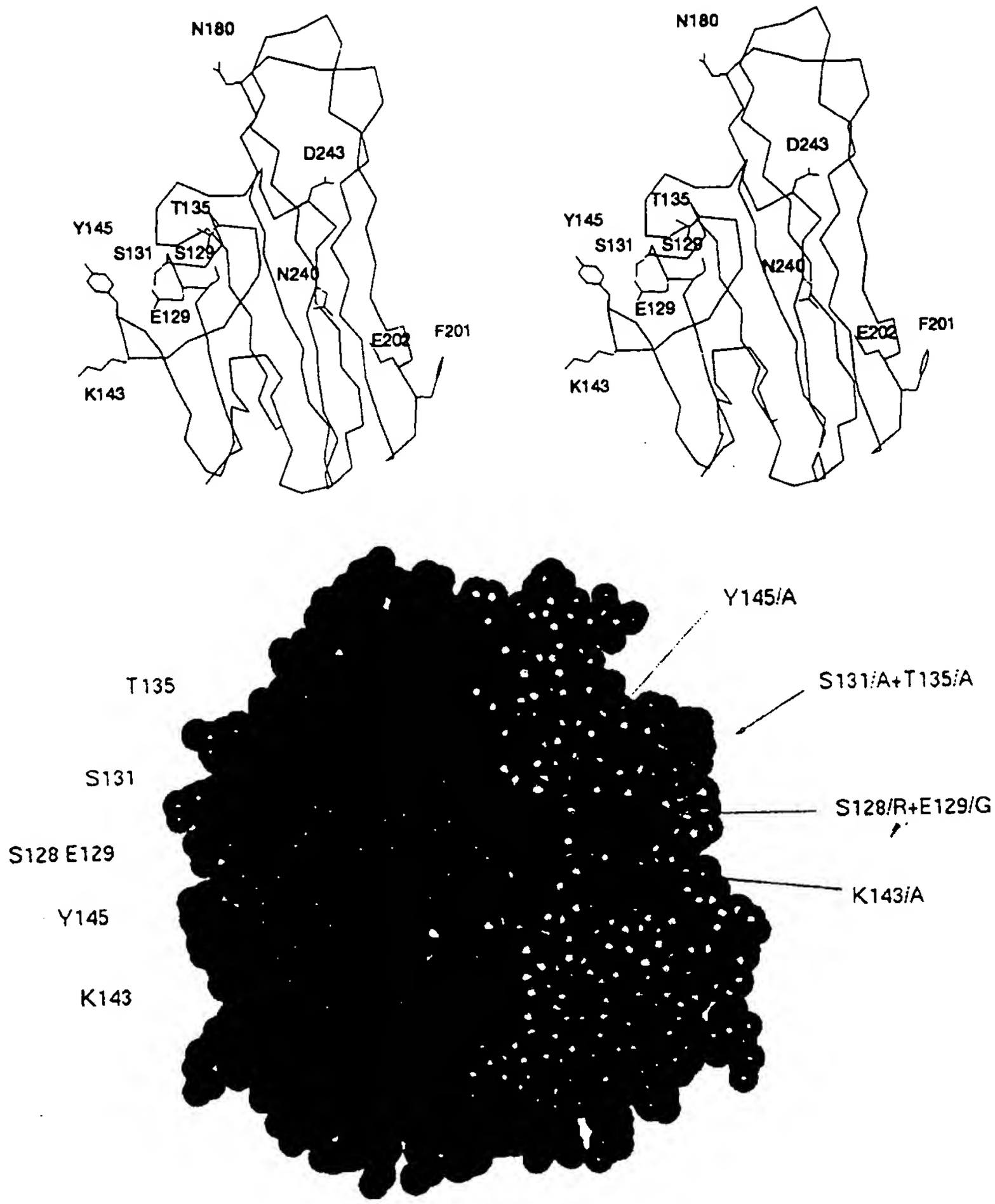

FIGURE 10: Mapping of gp39 residues targeted for site-directed replacement. (A, top) Stereo representation (α-carbon trace) of a monomer of the gp39 model. The side chains of all residues in gp39 selected for mutagenesis are shown in red and are labeled. (B, bottom) Space-filling model of the predicted gp39 trimer. Residues whose substitution with alanine did not affect gp39 binding to CD40 are shown in green, and residues whose substitution affected binding are shown in magenta. The amino acids mutated in a naturally occurring mutant of gp39 from a patient with X-HIM are shown in red.

wild-type gp39 in both binding assays. This result suggests that, as in the case of TNF-β, the residue at this position is not involved in receptor−ligand contacts and that substitution of E129 with glycine results in perturbations of the gp39 structure.

Then we examined the ability of these mutants to bind our panel of five different anti-gp39 mAbs. We found that both gp39−E129/G and gp39−E129/A were recognized by all the antibodies, with one exception, mAb 39−1.59. These data suggest that the epitope recognized by mAb 39−1.59 includes E129. In addition, binding of the antibodies to gp39−E129/G was much weaker than the binding to gp39−E129/A. This observation further suggests that the structure of this gp39 mutant is perturbed by the introduction of a glycine residue at this position. This contrasts with the observation that gp39-S128/R was not recognized by any of the antibodies in the panel. We conclude that mutations at both S128 and E129 in the gp39 expressed by this X-HIM patient contribute to lack of CD40 binding but that the mutation S128/R by itself is detrimental.

We have summarized our findings on the location of predicted gp39 surface residues involved in CD40 binding in Figure 10. In Figure 10B a subset of the residues which were targeted for substitution and which do not contribute to CD40 binding are shown in green. Those which, when substituted, result in mutant proteins with diminished CD40 binding are shown in magenta, and those found in the naturally occurring mutant from the X-HIM patient examined in this study are shown in red.

Although the database of gp39 and CD40 mutants must be significantly increased before firm conclusions can be drawn regarding the gp39−CD40 interaction, the data presented in this study suggest that the molecular contacts underlying gp39−CD40 binding bear significant similarity to those found in the TNF-β/TNFR system (Banner et al., 1993). However, there are some differences, suggesting that these two ligand−receptor systems utilize spatially overlapping but nonidentical and nonconserved sets of contact residues with different molecular determinants of binding. This may provide a common theme of receptor−ligand

binding for members of this protein family and allow for receptor−ligand specificity.

The critical role of the gp39−CD40 receptor−ligand pair in T_h−APC interactions suggests that molecules designed to inhibit or enhance this interaction would be potent immune modulators by mediating immune suppression or stimulation, respectively. Studies such as the one presented herein should provide the basis for understanding CD40−gp39 interactions at the molecular level.

ACKNOWLEDGMENT

We thank Dr. R. Mittler for providing the BMS-10 cell line, Dr. J. Ledbetter for providing mAbs G28-5 and 53-6, Tanya Spoon for excellent technical support, and Debby Baxter for help in preparing the manuscript. The contribution of the first three authors should be considered equal.

REFERENCES

Alderson, M. R., Armitage, R. J., Tough, T. W., Strockbine, L., Fanslow, W. C., & Spriggs, M. K. (1993) *J. Exp. Med. 178*, 669.

Allen, R. C., Armitage, R. J., Conley, M. E., Rosenblatt, H., Jenkins, N. A., Copeland, N. G., Bedell, M. A., Edelhoff, S., Disteche, C. M., Simoneaux, D. K., Fanslow, W. C., Belmont, J., & Spriggs, M. K. (1993) *Science 259*, 990.

Armitage, R. J., Fanslow, W. C., Strockbine, L., Sato, T. A., Clifford, K. N., Macduff, B. M., Anderson, D. M., Gimpel, S. D., Davis-Smith, T., Maliszewski, C. R., Clark, E. A., Smith, C. A., Grabstein, K. H., Cosman, D., & Spriggs, M. K. (1992) *Nature 357*, 80.

Aruffo, A., Stamenkovic, I., Melnick, M., Underhill, C. B., & Seed, B. (1990) *Cell 61*, 1303.

Aruffo, A., Farrington, M., Hollenbaugh, D., Li, X., Milatovich, A., Nonoyama, S., Bajorath, J., Grosmaire, L. S., Stenkamp, R., Neubauer, M., Roberts, R. L., Noelle, R. J., Ledbetter, J. A., Francke, U., & Ochs, H. D. (1993) *Cell 72*, 291.

Aruffo, A., Hollenbuagh, D., Wu, L., & Ochs, H. D. (1994) *Curr. Opin. Hematol. 1*, 12.

Bajorath, J., Stenkamp, R., & Aruffo, A. (1993) *Protein Sci. 2*, 1798.

Banner, D. W., D'Arcy, A., Janes, W., Gentz, R., Schoenfeld, H.-J., Broger, C., Loetscher, H., & Lesslauer, W. (1993) *Cell 73*, 431.

Callard, R. E., Armitage, R. J., Fanslow, W. C., & Spriggs, M. K. (1993) *Immunol. Today 14*, 559.

Clark, E. A., & Ledbetter, J. A. (1986) *Proc. Natl. Acad. Sci. U.S.A. 83*, 4494.

Di Santo, J. P., Bonnefoy, J. Y., Gauchat, J. F., Fischer, A., & de Saint-Basile, G. (1993) *Nature 361*, 541.

Durandy, A., Schiff, C., Bonnefoy, J. Y., Forveille, M., Rousset, F., Mazzei, G., Milili, M., & Fischer, A. (1993) *Eur. J. Immunol. 23*, 2294.

Durie, F. H., Fava, R. A., Foy, T. M., Aruffo, A., Ledbetter, J. A., & Noelle, R. J. (1993) *Science 261*, 1328.

Eck, M. J., & Sprang, S. R. (1989) *J. Biol. Chem. 264*, 17595.

Eck, M. J., Ultsch, M., Rinderknecht, E., de Vos, A. M., & Sprange, S. R. (1992) *J. Biol. Chem. 267*, 2119.

Foy, T. M., Shepherd, D. M., Durie, F. H., Aruffo, A., Ledbetter, J. A., & Noelle, R. J. (1993) *J. Exp. Med. 178*, 1567.

Fuleihan, R., Ramesh, N., Loh, R., Jabara, H., Rosen, R. S., Chatila, T., Fu, S. M., Stamenkovic, I., & Geha, R. S. (1993) *Proc. Natl. Acad. Sci. U.S.A. 90*, 2170.

Graf, D., Korthauer, U., Mages, H. W., Senger, G., & Kroczek, R. A. (1992) *Eur. J. Immunol. 22*, 3191.

Hermann, P., Blanchard, D., de Saint-Vis, B., Fossiez, F., Gaillard, C., Vanbervliet, B., Briere, F., Banchereau, J., & Galizzi, J.-P. (1993) *Eur. J. Immunol. 23*, 961.

Ho, S. N., Hunt, H. D., Horton, R. M., Pullen, J. K., & Pease, L. R. (1989) *Gene 77*, 51.

Hollenbaugh, D., Grosmaire, L. S., Kullas, C. D., Chalupny, N. J., Braesch-Andersen, S., Noelle, R. J., Stamenkovic, I., Ledbetter, J. A., & Aruffo, A. (1992) *EMBO J. 11*, 4313.

Hollenbaugh, D., Bajorath, J., Stenkamp, R., & Aruffo, A. (1993) *Biochemistry 32*, 2960.

Hollenbaugh, D., Ochs, H. D., Noelle, R. J., Ledbetter, J. A., & Aruffo, A. (1994) in *Immunological Reviews* (Moller, G., Ed.) pp 1−37, International Publishers, Ltd., Copenhagen.

Jin, L., Fendly, B. M., & Wells, J. A. (1992) *J. Mol. Biol. 226*, 851.

Jones, E. Y., Stuart, D. I., & Walker, N. P. (1989) *Nature 338*, 225.

Korthauer, U., Graf, D., Mages, H. W., Briere, F., Padayachee, M., Malcolm, S., Ugazio, A. G., Notarangelo, L. D., Levinsky, R. J., & Kroczek, R. A. (1993) *Nature 361*, 539.

Lane, P., Traunecker, A., Hubele, S., Inui, S., Lanzaveccia, A., & Gray, D. (1992) *Eur. J. Immunol. 22*, 2573.

Lane, P., Brocker, T., Hubele, S., Padovan, E., Lanzavecchia, A., & McConnell, F. (1993) *J. Exp. Med. 177*, 1209.

Lederman, S., Yellin, M. J., Krichevsky, A., Belko, J., Lee, J. J., & Chess, L. (1992) *J. Exp. Med. 175*, 1091.

Lederman, S., Yellin, M. J., Cleary, A. M., Pernis, A., Inghirami, G., Cohn, L. E., Covery, L. R., Lee, J. J., Rothman, P., & Chess, L. (1994a) *J. Immunol 152*, 2163.

Lederman, S., Yellin, M. J., Cleary, A.M., Pernis, A., Inghirami, G., Cohn, L. E., Covey, L. R., Lee, J. J., Rothman, P., & Chess, L. (1994b) *J. Immunol. 152*, 2163.

Noelle, R. J., Roy, M., Shepherd, D. M., Stamenkovic, I., Ledbetter, J. A., & Aruffo, A. (1992) *Proc. Natl. Acad. Sci. U.S.A. 89*, 6550.

Nonoyama, S., Hollenbaugh, D., Aruffo, A., Ledbetter, J. A., & Ochs, H. D. (1993) *J. Exp. Med. 178*, 1097.

Novotny, J., Bruccoleri, R. E., & Saul, F. A. (1989) *Biochemistry 28*, 4735.

Ochs, H. D., & Aruffo, A. (1993) *Current Opin. Pediatr. 5*, 684.

Paulie, S., Ehlin-Hendricksson, B., Mellstedt, H., Koho, H., Ben-Aissa, H., & Perlmann, P. (1985) *Cancer Immunol. Immunother. 20*, 23.

Smith, C. A., Farrah, T., & Goodwin, R. G. (1994) *Cell 76*, 959.

Spriggs, M. K., Armitage, R. J., Stockbine, L., Clifford, K. N., Macduff, B. M., Sato, T. A., Maliszewski, C. R., & Fanslow, W. C. (1992) *J. Exp. Med. 176*, 1543.

Stamenkovic, I., Clark, E. A., & Seed, B. (1988) *EMBO J. 7*, 1053.

Van den Eertwegh, J. M., Noelle, R. J., Roy, M., Shepherd, D. M., Aruffo, A., Ledbetter, J. A., Boersma, W. J. A., & Claasen, E. (1993) *J. Exp. Med. 178*, 1555.

Van Ostade, X., Tavernier, J., & Fiers, W. (1994) *Protein Eng. 7*, 5.

Villa, A., Notarangelo, L. D., DiSanto, J. P., Macchi, P. P., Strina, D., Frattini, A., Lucchini, F., Patrosso, C. M., Gilliahni, S., Mantuano, E., Agosti, S., Nocera, G., Kroczek, R. A., Fischer, A., Ugazio, A. G., de Saint Basile, G., & Vezzoni, P. (1994) *Proc. Natl. Acad. Sci. U.S.A. 91*, 2110.

Walz, G., Aruffo, A., Kolanus, W., Bevilacqua, M., & Seed, B. (1990) *Science 250*, 1132.

BI941956N